Journal of Natural Fibers

ISSN: (Print) (Online) Journal homepage: https://www.tandfonline.com/loi/wjnf20

Design, Fabrication, and Testing of a Raspador for Simultaneous Extraction and Brushing of Sisal Fibers by Small-scale Sisal Farmers

N. W. Barasa, K. D. Njoroge & T. O. Mbuya

To cite this article: N. W. Barasa, K. D. Njoroge & T. O. Mbuya (2021): Design, Fabrication, and Testing of a Raspador for Simultaneous Extraction and Brushing of Sisal Fibers by Small-scale Sisal Farmers, Journal of Natural Fibers, DOI: 10.1080/15440478.2021.1975597

To link to this article: https://doi.org/10.1080/15440478.2021.1975597

Published online: 06 Oct 2021.

Submit your article to this journal

Article views: 21

View related articles

View Crossmark data

Full Terms & Conditions of access and use can be found at
https://www.tandfonline.com/action/journalInformation?journalCode=wjnf20

JOURNAL OF NATURAL FIBERS
https://doi.org/10.1080/15440478.2021.1975597

Taylor & Francis
Taylor & Francis Group

Check for updates

Design, Fabrication, and Testing of a Raspador for Simultaneous Extraction and Brushing of Sisal Fibers by Small-scale Sisal Farmers

N. W. Barasa, K. D. Njoroge, and T. O. Mbuya

Department of Mechanical and Manufacturing Engineering, University of Nairobi, Nairobi, Kenya

ABSTRACT

Demand for natural fibers is on the rise as awareness of environmental protection keeps abreast. Sisal fibers, for instance, are largely utilized not only in the manufacture of mats, ropes, carpets, and sacks but also in the reinforcement of polymer composites. With the increased demand for sisal fibers, there is a need to equally increase the exploitation of sisal by small-scale farmers. UNIDO, for instance, recommended that appropriate small-scale machines that are accessible to small-scale holders should be developed. This research examines the progress in the development of small-scale machines and designs a raspador for simultaneous extraction and brushing of sisal fibers. This is to ensure that there is value and income addition for the small-scale farmers in East Africa and perhaps the rest of the world.

摘要

随着环保意识的不断提高,对天然纤维的需求正在上升. 例如,剑麻纤维不仅大量用于制造垫子、绳索、地毯和麻袋,而且还用于增强聚合物复合材料. 随着对剑麻纤维需求的增加,同样需要增加小农户对剑麻的开发. 例如,工发组织建议开发适合小规模持有者使用的小型机器. 本研究考察了小型机械的发展进展,并设计了同时提取和刷洗剑麻纤维的拉斯帕刀. 这是为了确保东非和世界其他地区的小规模农民获得价值和收入增加.

KEYWORDS

Raspador; design; fabrication; testing; sisal fibers; extraction; brushing

KEYWORDS

关键词; 拉斯帕多; 设计; 制作; 测试; 剑麻纤维; 提取; 疾驰的

Introduction

Sisal owes its origin to Yucatan State, Mexico (Kithiia, Munyasi, and Mutuli 2020). Its fiber is among the natural fibers with the highest mechanical properties. The plant grows well in regions with very minimal rainfall like the arid lands (Kayumba et al. 2007). It has many applications; for instance, sisal sap is used for production of biogas, its waste is used as animal fodder and its fiber is used in reinforcement of polymer composites and weaving of mats, ropes, carpets, and sacks (Kithiia, Munyasi, and Mutuli 2020; Majesh and Pitchaimani 2016).

Sisal plants are mostly grown on estates in East Africa (FAO 2013). However, UNIDO found that a substantial amount of sisal is also grown on small scale along the farm hedges in East Africa (UNIDO 2001). In 2003, while sisal estates in Kenya contributed 20,000 MT of the exports, small-scale sisal holders only contributed 5,000 MT because the majority of hedge sisal in East Africa is unexploited (EPZ 2005). The lack of appropriate technology is a significant impediment to the small-scale farmers in East Africa, who resort to using tedious and low yielding manual methods (Barasa, Njoroge, and Mbuya 2021; Oduori 2016). On the other hand, sisal from estates is processed using large-scale automatic decorticators in a process that is expensive and inaccessible to the small-scale farmers. The large-scale technology is uneconomical to the small-scale farmers, consumes a lot of water, and

CONTACT N. W. Barasa nelsonlyton@gmail.com Department of Mechanical Engineering, University of Nairobi, Nairobi, Kenya

© 2021 Taylor & Francis

poses an environmental concern (Oduori 2016). Hence, UNIDO recommended for the development of appropriate small-scale machines for exploitation of the large amounts of hedge sisal prevalent in the East African Region (UNIDO 2001).

Small-scale farmers in Brazil rely heavily on small-scale technology that has revamped the sisal industry, making it the leading producer of sisal fiber in the world (Cantalino, Torres, and Silva 2015). These small-scale machines can only extract sisal fibers; hence, brushing and baling are subsequently carried out in the warehouses. Based on a case study on Brazilian system, a small-scale machine was designed for small-scale farmers in Tanzania (Brenters 2000). This study investigated if it is possible to crush and extract the sisal fibers using human power. Since the machine required 1600 W against 200 W produced by a fully grown adult in a single day, it was impossible to crush and extract using human power (Brenters 2000; Van and Toussaint 1994). Moreover, all crushing tests failed and the machine could only extract or brush at a given time. Additionally, the machine produced excessive tow (Brenters 2000).

Another design was developed for small-scale farmers in Tanzania by Kawongolo, Sentong-Kibalama, and Brown (2002). This machine, however, was only designed for extraction, and the research recommended that washing and brushing are required to improve fiber qualities. The capacity and design efficiency of the machine were 12 $kghr^{-1}$ and 42.9%, respectively

Another design of the machine was developed for farmers in East Africa by Oduori (2002). This research recommended two important parameters for better extraction qualities, a speed of 1000 rpm and a gap size of 2 mm. However, this machine was only designed for extraction. Kanogu, Osore, and Kiguru (2011) designed a field model of the Oduori's (2002) design. They also did not address the issue of fiber brushing, and few tests were carried out to report on any machine ergonomics. Snyder et al. (2006) developed a modified version of the small-scale machine with a vertical feeding mechanism. This design did not include a brushing unit, and extensive tests were also not done to obtain conclusive results (Snyder et al. 2006). Naik, Swamy, and Naik (2014) also designed a small-scale machine and obtained a capacity of 10 $kghr^{-1}$. This machine was specifically used for extraction of Areca fibers.

Ahmad et al. (2017) designed and produced a small-scale sisal fiber extracting machine for farmers in Pakistan. This design achieved a capacity of 15.94 $kghr^{-1}$ of dry fiber and consumed 3.1 kW of power on average (Ahmad et al. 2017). This machine met the minimum recommended capacity of between 15 and 20 $kghr^{-1}$ for small-scale machines (Cantalino, Torres, and Silva 2015). The dry fiber content of the machine was 3.2%. However, similar to the previous designs, the machine was only designed for extraction.

Good-quality sisal fiber is obtained through a process that involves harvesting, extracting, drying, brushing, and bailing. And even though brushing is equally an important exercise needed to improve fiber quality, many of the small-scale machines developed so far are primarily concerned with extraction. Because of this, the targeted small-scale farmers still have to sell their fibers, while unbrushed (UHDS grade) (LSA (London Sisal Association) 2016) to merchants/traders who subsequently brush the fibers in their warehouses to improve the quality to UG grade. This implies that the farmers lose an income due to unbrushed fibers. Another option is for small-scale farmers to invest in another machine for brushing. However, this is most unlikely given their low financial capacity and often resort to manual extraction to earn a living.

This current research was carried out with the objective of addressing this gap by designing, fabricating, and testing an affordable and readily available raspador for extraction and brushing of sisal fibers. This machine will increase the exploitation of hedge sisal and the income of small-scale farmers.

Materials and methods

Materials

Design software: Inventor Professional 2018 from Autodesk Inc. was required for the design of the raspador.

Fabrication machines: a center lathe for machining of drum, shaft, and side discs; Radial drilling machine for indexing and drilling of fastening holes on the periphery of the drum; Power saw, guillotine, and nibbler machines for cutting of metal bars and sheets; Arc and gas welding machines for welding and gas cutting, respectively.

Fabrication materials: ANSI/ASME B36.10 standard pipe of 273.1 mm outer diameter; mild steel angle plates (50 mm by 50 mm by 3 mm) for fabrication of machine frame; mild steel sheet 2 mm thick for fabrication of drum cover, chute, and pulley guards; mild steel bar 6 mm thick for fabrication of anvils; UCP205 cast iron pillow block and other materials described in Table 1.

Sisal leaves: 3-year-old sisal from small-scale farmers in Nairobi, Kenya.

Tachometer and wattmeter for measuring drum speed and power consumption, respectively.

Methodology

The small-scale machine was conceptualized based on the raspador principle (UNIDO 2001). Kinematic analysis (Figure 1 a)) and kinetic analysis (Figure 3) were conducted to design the main components of the raspador. It is assumed that the drum approaches the sisal leave at a speed c due to relative motion caused by feeding the leaf. The kinematic analysis establishes an equation that relates important design variables, such as speed, blades/elements, and gap size to the quality of extraction/brushing.

For a blade B_1, its positions at initial moment in time and time (t) was determined using laws of trigonometry (Figure 1 b)). The x and y positions were modeled using equations 1 and 2 respectively;

Table 1. Materials required for fabrication of the machine.

S/n	Item	Quantity	Specifications
1	Extraction/brushing drum	1	Standard mild steel pipe; 457.2 mm outer diameter, 400 mm long and 3 mm thick
2	Extraction blades	12	Mild steel angle bars; 38*38*5 mm and length of 5.06 m
3	Drum side discs	2	Fabricated from 12.7 mm thick mild steel plate to obtain circular disc with 263.3 mm and 25 mm external and internal diameters respectively.
4	Machine frame	1	Mild steel angle bars; 50*50*5 mm and length of 5.17 mm.
5	Anvil	2	Cast iron flat bar,380 mm long by 80 mm wide and 18 mm thick with a 2 mm top line fillet
6	Shaft	1	Hardened steel shaft 25 mm diameter and 560 mm long
7	Machine drum protective cover	1	2 mm thick hot rolled iron sheet
8	Motor plate	1	5 mm thick mild steel plate 250 mm by 200 mm
9	Machine stands	4	Rectangular mild steel hollow bars (60 by 60 mm and 6 mm thick)
10	Pulley & belt guard	1	2 mm thick hot rolled iron sheet
11	Pulleys	2	Aluminum alloy tapered pulleys (driven pulley 5.5 cm, 6.5 cm, 7.5 cm and 8 cm and driving pulley 11 cm, 13 cm, 13.3 cm and 16.4 cm pitch diameters)
12	Belt	1	3 V rubber belt
13	Chute	1	2 mm thick hot rolled iron sheet
14	Pillow block and bearing assembly	2	UCP205 Cast iron pillow block assembly with 25 mm bore diameter bearing
15	Motor	1	5.5 Hp motor.
16	Brushes		Mild steel pins and emery cloths
17	Fasteners	84	4 M14, 20 M8 and 60 M6 bolts, nuts and washers

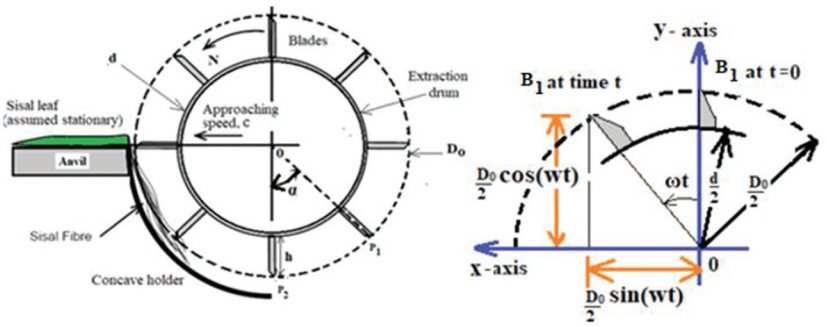

a) Raspador principle b) Position of blade B_1 at t = 0 and at time t

Figure 1. Raspador principle.

$$xB_1(t) = \begin{cases} 0, t = 0 \\ ct + \frac{D_0}{2}\sin(\omega t), timet \end{cases} \tag{1}$$

$$yB_1(t) = \begin{cases} \frac{D_0}{2}, t = 0 \\ \frac{D_0}{2}\cos(\omega t), timet \end{cases} \tag{2}$$

And similarly, for B_2;

$$xB_2(t) = \begin{cases} \frac{D_0}{2}\sin(-\alpha), t = 0 \\ ct + \frac{D_0}{2}\sin(\omega t - \alpha), timet \end{cases} \tag{3}$$

$$yB_2(t) = \begin{cases} \frac{D_0}{2}cos\alpha, att = 0 \\ \frac{D_0}{2}\cos(\omega t - \alpha), timet \end{cases} \tag{4}$$

The parameter ct accounts for the displacement due to speed (c) of the drum in time t. Letting $R = \frac{c}{\omega}$ (m/rads), equations 1 to 4 were simplified to equation 5 to 8.

$$xB_1(t) = \begin{cases} 0, t = 0 \\ R\omega t + R_0\sin(\omega t), timet \end{cases} \tag{5}$$

$$yB_1(t) = \begin{cases} R_0, t = 0 \\ R_0\cos(\omega t), timet \end{cases} \tag{6}$$

$$xB_2(t) = \begin{cases} R_0\sin(-\alpha), t = 0 \\ R\omega t + R_0\sin(\omega t - \alpha), timet \end{cases} \tag{7}$$

$$yB_2(t) = \begin{cases} R_0 cos\alpha, t = 0 \\ R_0\cos(\omega t - \alpha), timet \end{cases} \tag{8}$$

The tips of blades B_1 and B_2 strike the x-axis at time t_1 and t_2 respectively (Figure 2), and the difference in their displacement at this point yields a parameter that is termed as pitch in various studies (Brenters 2000; Oduori 2016). In this study, this value was referred to as delta (δ).

The values of xB_1 and xB_2 at times t_1 and t_2 respectively were established as follows;

$$y_{B_1}(t_1) = R_0 cos(\omega t_1) = 0$$

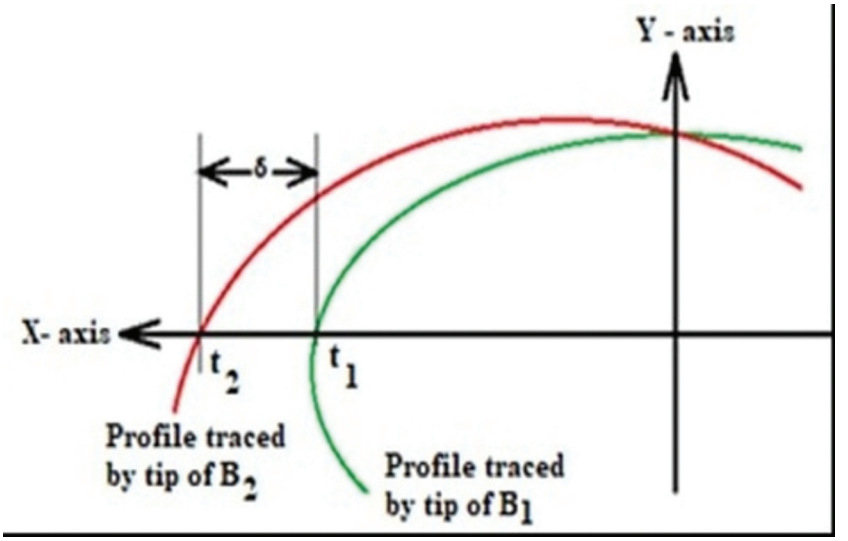

Figure 2. Profiles traced by tips of blades P1 and P2 in a quarter turn.

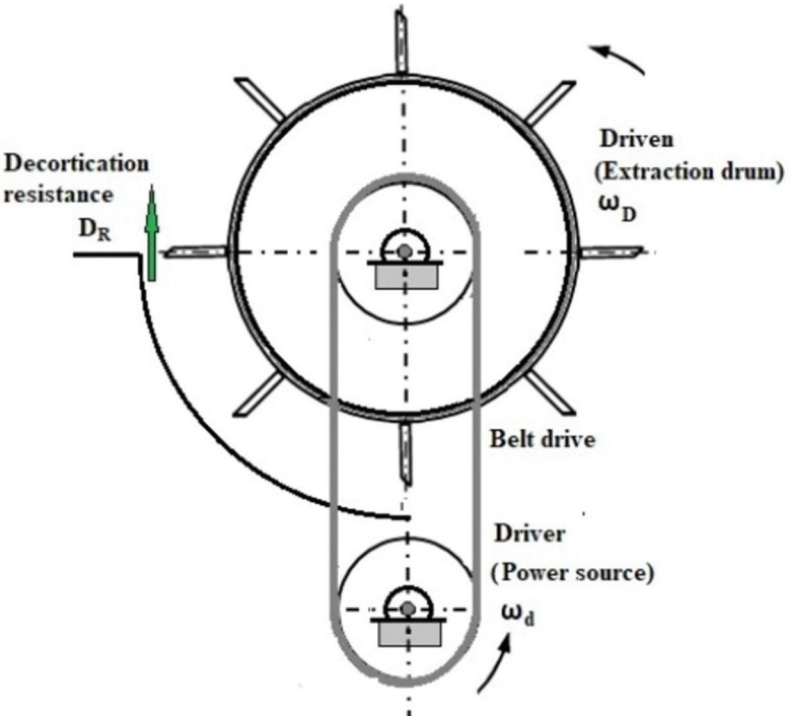

Figure 3. Model for kinetic analysis.

$$\omega t_1 = \frac{\pi}{2} \tag{9}$$

hence

$$xB_1(t_1) = Rt_1\frac{\pi}{2t_1} + R_0 sin\left(t_1\frac{\pi}{2t_1}\right)$$

$$= R\frac{\pi}{2} + R_0 \tag{10}$$

And

$$y_{B2}(t_2) = R_0\cos(wt_2 - \alpha) = 0$$

$$\omega t_2 = \frac{\pi}{2} + \alpha \tag{11}$$

hence

$$x_{B2}(t_2) = Rt_2\left(\frac{\pi + 2\alpha}{2t_2}\right) + R_0\sin\left(\frac{\pi + 2\alpha}{2t_2}t_2 - \alpha\right)$$

$$= \frac{R}{2}(\pi + 2\alpha) + R_0 \tag{12}$$

Therefore, δ was expressed by deducting equation 10 from equation 12;

$$\delta = \alpha R$$

$$\delta = \frac{2\pi}{n}\left(\frac{c}{\omega}\right) = \frac{2\pi c}{n\omega} \tag{13}$$

δ has been found by earlier research to vary inversely with the quality of extraction (Kanogu, Osore, and Kiguru 2011; Oduori 2002; Snyder et al. 2006). This was an important design equation for the machine since it relates the number of blades/elements, speed, and gap to decortication quality (δ).

Kinetic analysis was also conducted but since forces involved in raspador have been found to be negligible (Kanogu, Osore, and Kiguru 2011; Oduori 2002), this analysis was carried out with the aim of establishing the power requirements and decortication resistance (Figure 3). The energy involved in extracting a sisal leaf was estimated using equation 14 (Oduori 2002).

$$E = \omega R_O \int_{t_1}^{t_2} D_R(t)dt \tag{14}$$

where ω is the drum speed, R_0 radius at the tip of the blades, and D_R decortication resistance. Based on the mean value theorem, mean decortication resistance ($(D_R)_e$) was expressed by equation 15.

$$(D_R)_e = \frac{1}{t_2 - t_1}\int_{t_1}^{t_2} D_R(t)dt \tag{15}$$

$(D_R)_e$ was estimated by first modeling the leaf as a cantilever (Figure 4) and then applying the equations of maximum bending (Oreko et al. 2018).

Using equations 14, 15 and 16, the equation that relates the power consumption to the size and speed of the drum was established as equation 17.

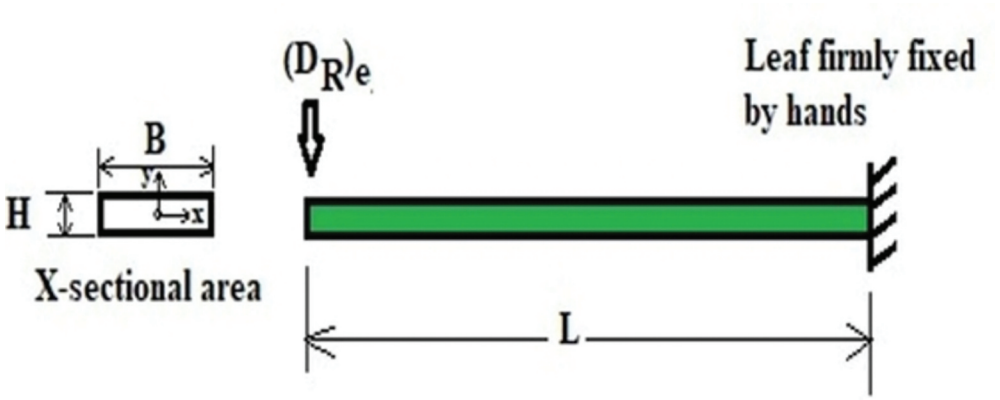

Figure 4. Cantilever model to determine decortication resistance.

$$P = \frac{E}{\Delta t} \tag{16}$$

$$= \frac{1}{t_2 - t_1} \omega R_O \int_{t_1}^{t_2} D_R(t)dt$$

$$= (D_R)_e \omega R_O \tag{17}$$

Equation 17 was used to appropriately size the motor and extraction drum. There was little information or principles concerning the brushing unit. Therefore, a brushing unit was also conceptualized based on the raspador principle and improved during brushing in a trial and error approach. The kinematic and kinetic analyses used for extraction unit were equally employed in designing the brushing unit. However, for brushing unit, the brushing elements comprised of blunt blades, steel comping pins and plastic brushes. This unit was to be evaluated and optimized through thorough testing. The two units were designed to use common primary units to save on cost. Equations 13 and 17 were then used as a basis to design the various parts of the machine. A combined drum was selected to reduce the overall weight of the machine. ANSI/ASME B36.10 standard mild steel pipe of 273.1 mm outer diameter was preferred.

A minimum output of 15 kgh^{-1} (Oduori 2002) was employed in approximating the feeding velocity (c). The power required to extract and brush a sisal leaf was theoretically estimated to be the size of a suitable motor. The torques on the shaft were modeled using Figure 5.

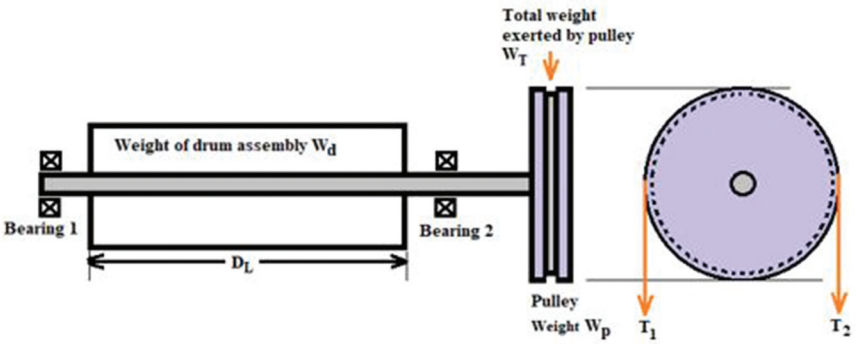

Figure 5. Sketch of shaft design.

The shaft was then designed based on Guest's (equation 18) and Rankine's (equation 19) failure theories.

$$\frac{\pi}{16} * \tau_{max} * d^3 = \sqrt{(K_m * M_{max})^2 + (K_t + T)^2} \tag{18}$$

$$\frac{\pi}{32} * \sigma_b * d^3 = \frac{1}{2}\left\{K_m * M_{max} + \sqrt{(K_m * M_{max})^2 + (K_t * T)^2}\right\} \tag{19}$$

where;

M_{max} – highest bending moment on the shaft
K_m– combined bending shock and fatigue factor
K_t– combined torsional shock and fatigue factor
τ_{max}- maximum shear stress permitted
σ_b- highest normal stress that the shaft material can handle
T – torque

A standard V belt was selected because it transmits high power and has little slip (Shigley, Mischke, and Brown 2004). Therefore, belt length, center distance, and pulley diameters selected were then factored in during the design and sizing of the chute, machine frame, drum cover, and belt guard. The conceptualized design was then drafted using Inventor Professional 2018 software. The ANSI/ASME standard parts selected and other materials were locally acquired and used to fabricate the machine at the Mechanical Engineering Workshop, University of Nairobi.

The fabricated machine was extensively evaluated in the laboratory at the university and in a hedge sisal field at Kasarani, in Nairobi county, Kenya. To determine power consumption, the drum speed was varied from 960 rpm to 1615 rpm at 1 mm gap size and 12 blades/brushing elements using the tapered pulleys. At a given drum speed, 6 samples were extracted and brushed. To determine the quality of sisal fibers during extraction while holding other variables constant, 6 sisal samples were extracted at varying gap sizes (1.0, 1.5, 2.0, 2.5, 3.0, and 3.5 mm), blades (3, 6, and 12), and drum speed (900–1400 rpm). Weight, color, and fiber lengths were recorded immediately after extraction and drying. After 3 days of direct sun drying, the extracted fibers were also brushed at varying drum speed, gap size, and number of brushing elements. Equally, the weight, color, and fiber length were recorded before and after brushing. Extensive data collection was used to evaluate the performance of the machine and to optimize the raspador design. Equation 20 was used in determining the spread of the data obtained.

$$\sigma = \sqrt{\frac{1}{N}\sum_{i=1}^{N}(x_i - \mu)^2} \tag{20}$$

where;

σ – SD
N – Population size
x_i – ith data value
μ – Average

Results and discussion

Implications of the kinematic analysis

The literature study established that δ inversely related to quality of extraction (Oduori 2002). Moreover, this study further establishes that it also inversely relates to the brushing quality. δ only depends on feeding speed (c), extraction blades/brushing elements (n) and drum speed (ω). When δ is too large, it leads to poor extraction and brushing qualities. However, when δ is extremely small, it

leads to excessive crushing forces, breakage of sisal fibers and energy wastage. And since the value of δ does not depend on the size of the drum, the drum was designed as dictated by the overall size and weight desired and the available standard pipes. An experiment was therefore designed to optimize the values of speed, gap size, and number of blades/elements.

Implications of the kinetic analysis

The reported mean values of the properties of Kenyan sisal fiber (L = 150 cm, B = 12 cm, H = 3 cm, and E = 32.9 GN/m^2) (Phologolo et al. 2012) were utilized together with the equations of cantilever beam (Oreko et al. 2018) to estimate the maximum bending moment and decortication resistance used in the design process. The decortication resistance determined was 118.44 N. Using the elastic modulus of mild steel found in the literature, it was determined that the maximum bending force of a blade measuring 38 mm by 38 mm by 3 mm and 400 mm long can be supported is 15,499.7 N. This value was much more than the resistance force offered by a sisal leaf; therefore, the kinetic analysis was aimed at determining the power consumption and size of the motor.

An average drum speed of 1000 rpm as applied in the previous designs (Ahmad et al. 2017; Oduori 2002) and pipe diameter of 200 mm and (D_R)e determined were used to determine the power consumption as 2.84 Hp for both units. The idling power accounted for 57% of the total power (Oduori 2002) hence it was economical to design a machine that could extract and brush simultaneously to save on idling power consumed irrespective of the operation. In raspador, the power source accounts for 60% of the total cost (Oduori 2002) and hence, to minimize on cost, a 3 Hp motor was selected.

Design of the belt drive (Figure A6)

Belt drive being quiet, flexible, cheap, and appropriate for low-torque and high-speed designs was preferred for gear drive (Shigley, Mischke, and Brown 2004). It was designed based on the ISO4184 standard and Roulunds design charts (Roulunds 2004). A power rating (P_m) of 3 Hp, 1500 rpm, and 1000 rpm driving (N_1) and driven (N_2) speed, respectively, 148.05 N extraction resistance, and a service time of 10 hours per working day were used to design the belt drive. Using these data, it was established from design charts that the service factor C_1 for this machine was 1.4. The design power was 3.089 kW and with a drum speed of 1500 rpm, a 3 V belt was most suitable. Using a speed ratio of 1.5, the datum diameter of the larger pulley was estimated at 225 mm when a 150 mm diameter smaller pulley was selected. The center distance (Cs) desired for small machines needs to be between 262 mm and 748 mm as determined from equation 21.

$$0.7\left(d_p + D_d\right)mm < Cs < 2\left(d_p + D_d\right)mm \tag{21}$$

A center distance of 500 mm was therefore assumed during the initial trials. From equation 22, the belt length was determined to be 1589.9 mm. However, the nearest ISO 4184 standard belt length selected was 1587 mm. This reduced the actual center distance to 498.5 mm.

$$L_d = 2C_s + 1.57\left(d_p + D_d\right) + \frac{\left(D_d - d_p\right)^2}{4C_s}(mm) \tag{22}$$

A belt speed of 11.67 m/s was determined using equation 23. This speed was less than the maximum recommended speed for 3 V belts of 40 m/s hence suitable for this design

$$V_b = \frac{d_p * N_1}{19100}\left(ms^{-1}\right) \tag{23}$$

Moreover, the deflection frequency (equation 24) was 14.71 Hz with 2 pulleys, 11.67 m/s belt speed (v), and 1587 mm belt length (L_d). The maximum allowable frequency is 100 Hz for 3 V belts.

$$f = \frac{a * v * 1000}{L_d} \tag{24}$$

From Roulunds (2004) belt drive design manual, the power rating per 3 V belt was 4.89 kW for drum speed of 1500 rpm, small pulley datum diameter of 150 mm, and speed ratio of 1.5. Moreover, it was determined that; with a belt length correction factor (C_2) of 0.9986, arch and angle of contact correction factor (C_3) of 0.99, only one belt was required (equation 25).

$$z = \frac{P_M * C_1}{P_N * C_2 * C_3} \tag{25}$$

Belt tension (equation 26) was 180 N/belt with tension factor K_1 and centrifugal factor K_2 of 1.746 and 0.095 kg/m, respectively (Roulunds 2004).

$$T_{stat} = 500 * K_1 * \frac{P_m}{zV} + K_2 * V^2 \left(\frac{\mathrm{N}}{\mathrm{belt}}\right) \tag{26}$$

The static and dynamics shaft loads were found to be 359 N and 334 N, respectively, and also determined from equations 27 and 28, respectively. These loads were used to dimension the shaft and the bearing units.

$$S_{stat} = 2 * z * T_{stat} * Sin\left(\frac{\beta}{2}\right)(\mathrm{N}) \tag{27}$$

$$S_{dyn} = 707 * \frac{P_m}{v} * \sqrt{K_1{}^2 + 1 - (K_1{}^2 - 1)Cos\beta}(\mathrm{N}) \tag{28}$$

Shaft design (Figure A7)

The weight of the drum assembly (W_d) was determined to be 300 N as the total weights of the drum, side discs, and the extraction/brushing elements. It was assumed to a lumped mass at point 2 of the shaft for simplification. The weight exerted by the pulley (W_T) was the pulley's weight and the belt tension (T_1 and T_2). Using standard pulley weight, the weight of the pulley was 83.4 N. The total tension force is either a static or dynamic load depending on which is the largest (Roulunds 2004). 359 N static load was the largest and, therefore, W_T was 442.4 N. Using these forces, force and bending moment diagrams were drawn (Figure 6).

The maximum bending moment (M_{max}) was 30.16 Nm. A torque of 21.07 Nm was also established using power expression (equation 29).

$$P = \frac{2\pi NT}{60} \tag{29}$$

Using Guest's and Rankine's failure theories, the minimum shaft diameter was established to be 16.6 mm and 16.15 mm, respectively. However, the minimum available ISO standard shaft selected was 25 mm diameter shaft. UCP205 pillow block with 25 mm bore was used because its static load and dynamic load capacities of 7,850 N and 14,000 N were more than required of 359 N and 334 N, respectively.

CAD drawings and fabrication

The design of the machine was generated using Inventor Professional 2018 Software; Figure 7 a) is an isometric view of the raspador generated using the software. Figure 7 b) is a view of the fabricated field model. More Cad drawings are as presented in Appendices, Figures A1–A7.

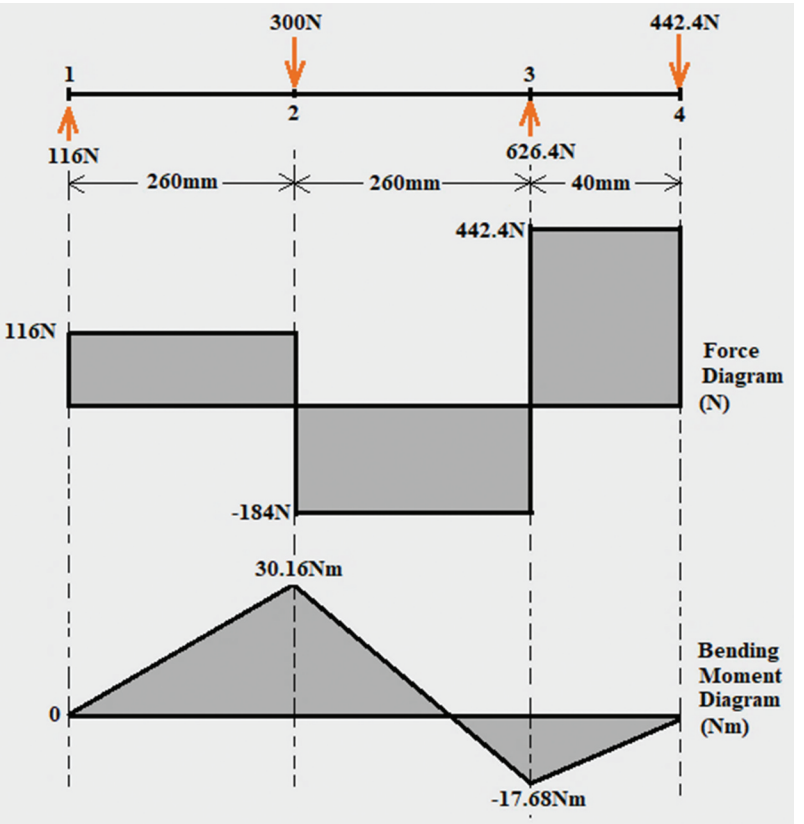

Figure 6. Force and bending moment diagram.

Drum speeds and variation of power consumption

The tapered pulleys yielded drum speed shown in Figure 8 using a fixed speed motor during laboratory tests.

The power consumed by the raspador was found to vary with drum speeds and gap size. The total power (TP), idling power (IP), Extraction power (EP), and Brushing power (BP) all increased with drum speed and slightly dropped with increase in gap size (Figure 9).

From equation 17, it was seen that the power consumed is directly related to the decoration resistance, drum speed, and drum radius. Therefore, the reduction in power consumption with increase in gap size is attributed to the reduced extraction/brushing resistances. The correlation coefficients of 0.993, 0.995, and 0.998 were established between total power consumption and drum speed at gap sizes of 1 mm, 2 mm, and 3 mm, respectively. This finding was important in the optimization of the raspador to ensure that the minimal possible drum speed was used.

The average power required to extract one sisal leaf was 1.368 kW better than that obtained by Ahmad et al. (2017) of 4.8 kW. Average power consumption for brushing per sisal leaf was 1.019 kW. However, the percentage increase in power consumption due to addition of brushing unit was only 16.8%. This is economical, unlike fabricating a different machine for brushing alone. IP is a major contributor to power consumption and is consumed whether the raspador is extracting, brushing, or running idle. Therefore, extracting and brushing at the same time saves on power consumption.

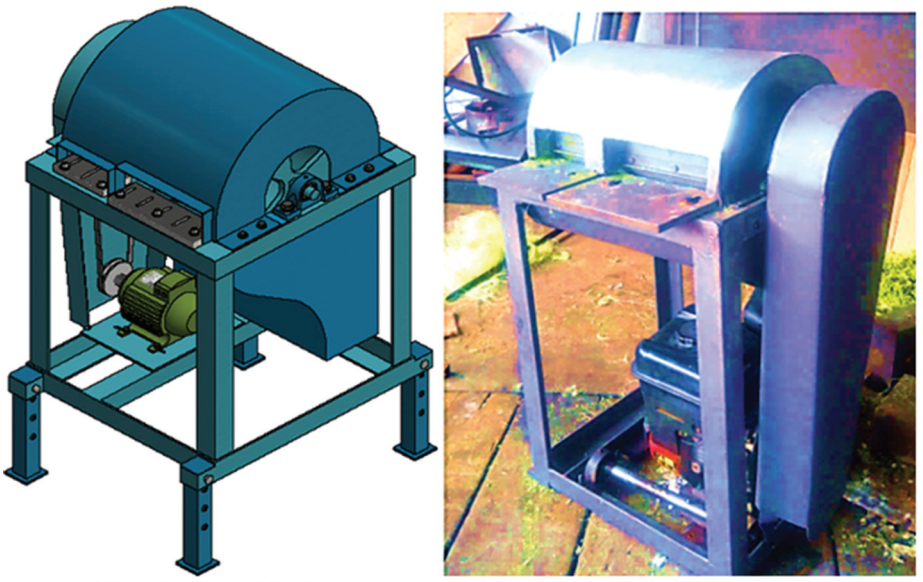

Figure 7. Raspador CAD drawing and fabricated views.

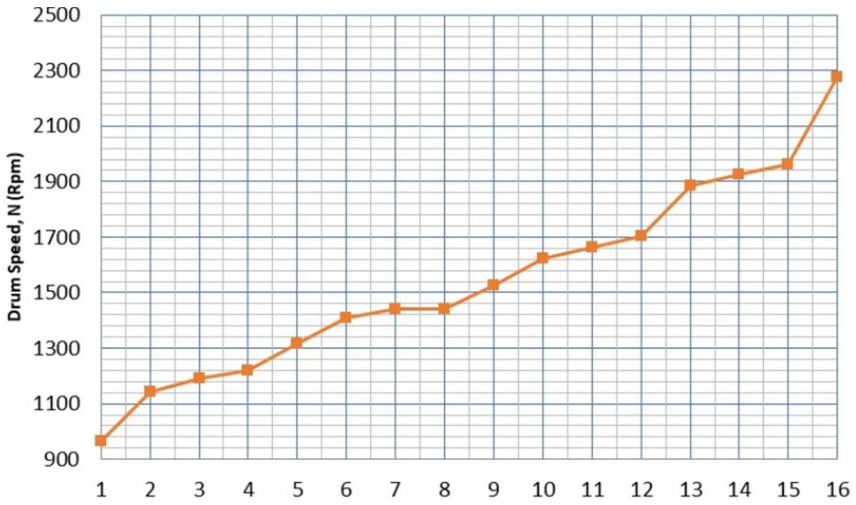

Figure 8. Drum speeds from speed ratios.

Fiber properties and machine capacity

The raspador's average wet and dry fiber yields were 11.94% and 5.03% respectively during extraction and dry fiber yield of 3.42% for the extraction unit. The extraction dry fiber yield was better than those reported by Ahmad et al. (2017) of 10.1% and 3.2% wet and dry fiber yields respectively. Moreover, Kawongolo, Sentong-Kibalama, and Brown (2002); Srinivasakumar et al. (2013); Naik, Swamy, and Naik (2014) reported 3.2%,3.0% and 3–5% dry fiber yields respectively.

A design efficiency of 39% was achieved by the machine as compared to 43% reported by Kawongolo, Sentong-Kibalama, and Brown (2002) if rationalized with a design capacity of 28 $kghr^{-1}$. An extraction capacity of 10.84 $kghr^{-1}$ was achieved by the machine. The capacity was comparable to 12 $kghr^{-1}$ achieved by Kawongolo, Sentong-Kibalama, and Brown (2002), 15.94

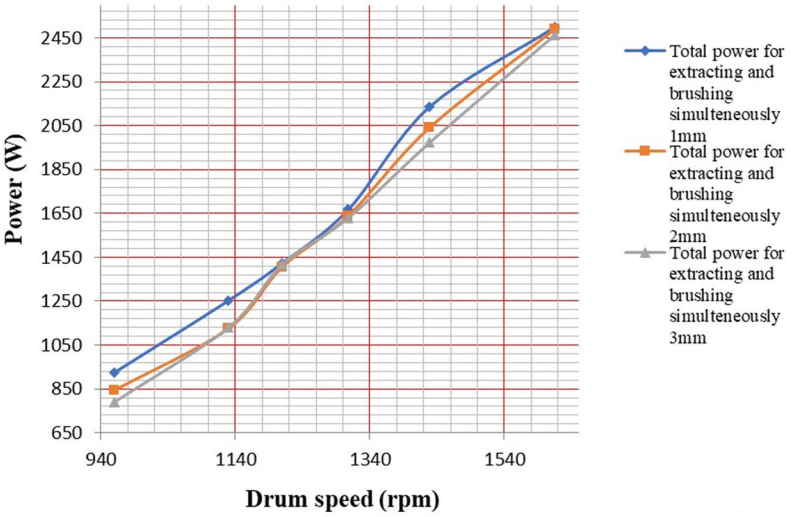

Figure 9. Power variation with gap sizes.

kghr^{-1} by Ahmad et al. (2017), 9–10 kghr^{-1} by Naik, Swamy, and Naik (2014) and 15–20 kghr^{-1} by Cantalino, Torres, and Silva (2015) whose machines could only extract. Although this machine had the advantage of performing both extraction and brushing simultaneously, its extraction capacity was comparable with other designs. In addition to this extraction capacity, the machine achieved a brushing capacity of 24.64 kghr^{-1}. A study that partly investigated on brushing did not report on the brushing capacity (Brenters 2000).

The average lengths and the color of the sisal fibers were used to assess the quality of fibers according to guidelines set by London Fiber Association (LSA (London Sisal Association) 2016). The length and color of fibers are used to classify the sisal fibers into grades 1, 2, 3 L, 3S, Under Grade (UG), Sub Standard Under Grade (SSUG) and Unwashed Hand Decorticated Sisal (UHDS) (LSA (London Sisal Association) 2016). The results indicated that the average lengths and the color of the fibers during extraction and brushing highly depend on the drum speed, gap size, and number of extraction blades/brushing elements. In this study, a variable called length ratio[1] (L_R) was used for comparison purposes. This ratio is directly related to the average fiber length. It was observed that during extraction and brushing L_R reduced with increase in drum speed (Table 2).

Table 2. Effect of speed on length ratio, color, and grade of sisal fibers.

Number of Blades/ elements	Gap Size (mm)	Drum speed (rpm)	Length ratio L_R		Fiber color		Fiber grade	
			Extraction	Brushing	Extraction	Brushing	Extraction	Brushing
12	2.5	900	0.940 ± 0.048	0.981 ± 0.015	Green	Brown	UHDS	SSUG
		1092	0.889 ± 0.026	0.960 ± 0.026	Green	Brown	UHDS	SSUG
		1200	0.880 ± 0.018	0.950 ± 0.033	White/ green	White and brown	UHDS	UG
		1325	0.872 ± 0.021	0.938 ± 0.012	White/ green	White and brown	UHDS	UG
		1400	0.869 ± 0.006	0.936 ± 0.006	White/ green	White and brown	UHDS	UG

Key: ± – Standard deviation for 6 sisal leaves
UHDS – Unwashed Hand Decorticated Sisal
UG – Under Grade
SSUG – Substandard Under Grade
L_R- Ratio of fiber length to leaf length for extraction or original fiber length for brushing

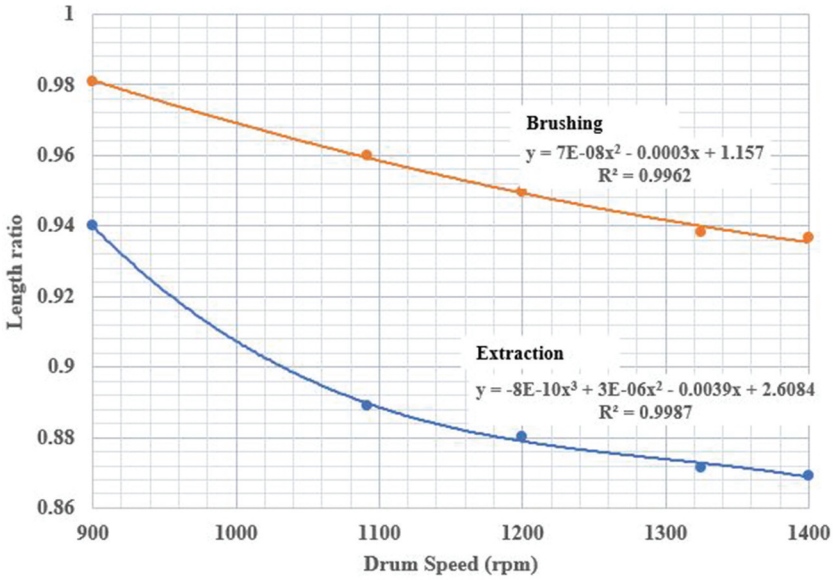

Figure 10. Variation of length ratio with drum speed.

Increasing drum speed from 900 to 1400 rpm at 12 blades/elements and 2.5 gap size reduces L_R by 7.6% and 4.6% for extraction and brushing, respectively. Correlation coefficients of 1 and 0.995 were established between L_R and drum speed for extraction and brushing, respectively (Figure 10).

An increase in drum speed increases the number of interactions between the blades/elements and sisal fibers, hence the blade/element stresses that debond the fiber hemicellulose and lignin matrix from the reinforcing cellulose microfibrils, leading to increased fiber breakage (Barasa, Njoroge, and Mbuya 2021). Moreover, the increased blade stresses lead to grinding of fiber cells, reducing cell crystallinity (Petroudy 2017) and strength, and this increases the fiber breakage. Furthermore, the increased forces damage the fiber cuticle introducing interfacial defects that exacerbate fiber breakage (Zhu, Hao, and Zhang 2018). Cumulatively, this causes the reduction of L_R with drum speed. The color, on the other hand, improved with speed (from green for extraction or brown for brushing to

Table 3. Effect of blades and elements on length ratio, color, and grade of sisal fibers

Drum speed (rpm)	Gap Size (mm)	Number of blades/ elements	Length ratio L_R		Fiber color		Fiber grade	
			Extraction	Brushing	Extraction	Brushing	Extraction	Brushing
1400	2.5	3	0.962.2 ± 0.018	0.990 ± 0.010	Green	Brown	UHDS	SSUG
		6	0.951 ± 0.017	0.980 ± 0.001	White/ green	White/ brown	UHDS	SSUG
		12	0.869 ± 0.006	0.940 ± 0.006	White/ green	White/ brown	UHDS	SSUG

Key: ± – Standard deviation for 6 sisal leaves
UHDS – Unwashed Hand Decorticated Sisal
UG – Under Grade
SSUG – Substandard Under Grade
L_R- Ratio of fiber length to leaf length for extraction or original fiber length for brushing

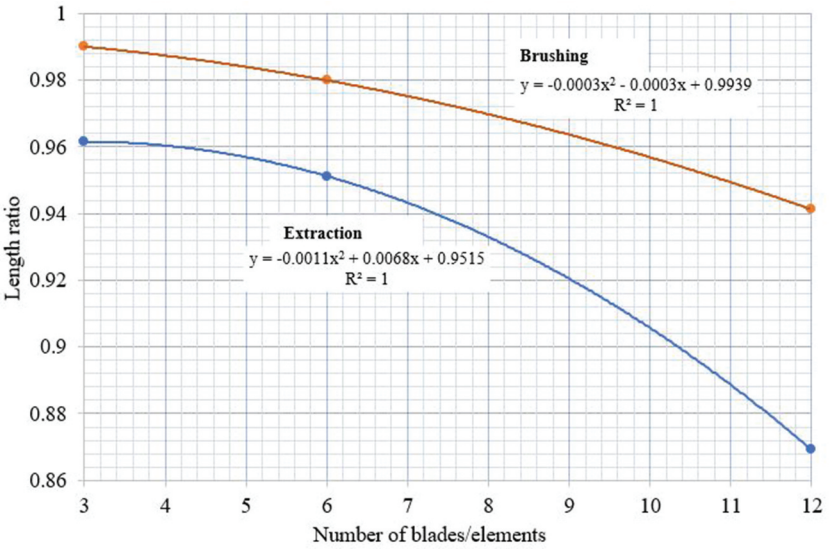

Figure 11. Variation of length ratio with blades and elements.

white). A good balance between fiber color and length, hence fiber quality, was obtained at drum speeds between 1000 and 1200 rpm for extraction but the grade remained UHDS. Similarly, brushing results optimized between 1000 and 1200 rpm drum speed and UG grade were obtained.

Similarly, L_R reduces with an increase in the number of extraction/brushing elements (see Table 3).

Increasing the blades/elements from 3 to 12 at 1400 rpm and 2.5 gap size reduces L_R by 9.7% and 5.1% for extraction and brushing, respectively. The increase in blades/elements equally increases the stresses on the fibers that debond the fiber hemicellulose and lignin matrix from the reinforcing cellulose microfibrils, increases grinding effect that reduces cell crystallinity and increases cuticle damage that contributes to fiber breakage and hence reduces L_R. Correlation coefficients for both extraction and brushing were unity (Figure 11). The color, however, improved from white-green (extraction) and brown-white (brushing) to white with increase in number of elements. Optimized values were obtained at 6 blades and 3 blades for extraction and brushing, respectively.

Table 4. Effect of gap size on length ratio, color, and grade of sisal fibers

Number of blades/ elements	Drum speed (rpm)	Gap Size (mm)	Length ratio L_R		Fiber color		Fiber grade	
			Extraction	Brushing	Extraction	Brushing	Extraction	Brushing
3	1400	1.0	0.947 ± 0.043	0.854 ± 0.028	White/ green	Cream white	UHDS	SSUG
		1.5	0.951 ± 0.020	0.899 ± 0.010	White/ green	Cream white	UHDS	UG
		2.0	0.959 ± 0.024	0.970 ± 0.022	Green	White/ brown	UHDS	UG
		2.5	0.962 ± 0.047	0.990 ± 0.016	White/ green	White/ brown	UHDS	SSUG
		3.0	0.970 ± 0.022	0.986 ± 0.013	Green	White	UHDS	UG
		3.5	0.961 ± 0.010	0.990 ± 0.012	Green	White	UHDS	UG

Key: ± – Standard deviation for 6 sisal leaves
UHDS – Unwashed Hand Decorticated Sisal
UG – Under Grade
SSUG – Substandard Under Grade
L_R- Ratio of fiber length to leaf length for extraction or original fiber length for brushing

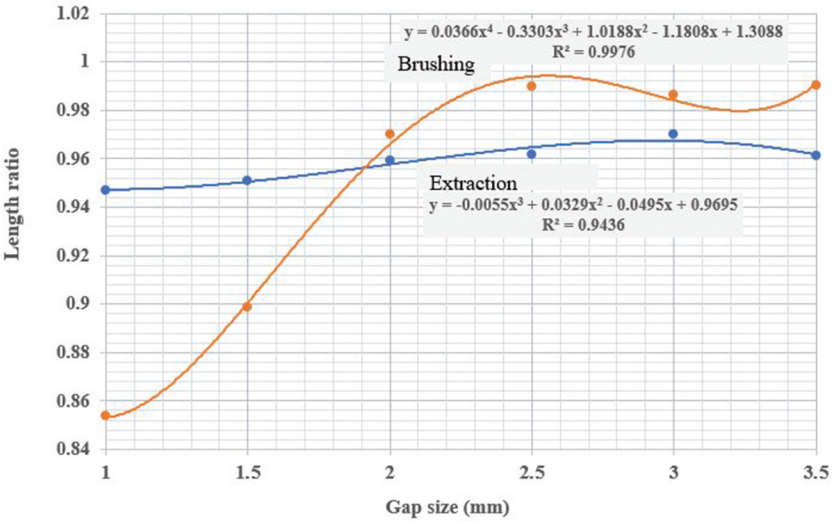

Figure 12. Variation of length ratio with gap size.

L_R, however, increased with gap size. Increasing gap size from 1 to 3.5 mm at 1400 rpm and 3 blades/elements increases L_R by 1.5% and 15.9% for extraction and brushing, respectively (Table 4).

An increase in gap size reduces the intensity of blade stresses that is known for debonding the fiber hemicellulose and lignin matrix from the reinforcing cellulose microfibrils, grinding the fiber cells (reduces cell crystallinity) and hence strengthens and damages the fiber cuticle by introducing interfacial defects that exacerbate fiber breakage. Therefore, increase in gap size increases fiber L_R. From Figure 12, the correlation coefficients of 0.97 and 1 during extraction and brushing, respectively, were obtained.

In contrast, the fiber color deteriorated with the increase in gap size (from white-green to green/brown (extraction) and white to dark brown (brushing)). This was due to incomplete decortication/brushing leaving a lot of undecorticated barks in the fiber hunk. Given that L_R and color were found to be inversely related and are both important fiber quality variables, there was a need to optimize the extraction and brushing variables for good-quality sisal fiber. The optimum quality for extraction was obtained using 6 blades, a gap size ranging between 1.5 and 2 mm and a speed ranging between 1000 and 1200 rpm. The brushing quality was optimized at 3 elements, a gap size of 2–3 mm, and a speed of between 1000 and 1200 rpm. Moreover, the addition of other brushing members such as steel pins helped in removing the tow and combing the sisal fibers. The effect of the pins on L_R was negligible. Another important observation was that brushing greatly improved the quality of the sisal fibers. This is because brushing refines the fibers by removing defective, short and curled fibers, and undecorticated barks from the fiber hunk (Barasa, Njoroge, and Mbuya 2021).

Conclusion

A raspador for simultaneous extraction and brushing of sisal fibers was designed, fabricated, and tested. The extraction and bushing capacities of the machine are 10.84 $kghr^{-1}$ and 24.64 $kghr^{-1}$ in that order. Its design efficiency is 39% with wet and dry yield contents of 6.44% and 3.62%, respectively, for extraction. The dry fiber yield is 3.42% for the brushing unit. The power consumption per sisal leaf is 1.37 kW during extraction and 1.02 kW during brushing. The quality of sisal fibers significantly depends on the drum speed, gap size, and number of blades or elements. Extraction quality is optimum at 6 blades, 1000 – 1200 rpm drum speed, and 1.5–2 mm gap size. Brushing quality is

optimum at 3 elements, 1000–1200 rpm drum speed, and 2–3 mm gap size. Lastly, brushing significantly improves the quality of the sisal fibers. In conclusion, more quantitative and qualitative informations on the effects of these raspadors on sisal fibers are detailed in a previous paper by Barasa, Njoroge, and Mbuya (2021).

Note

1. Ratio of the average fiber length to original leaf length

Acknowledgments

There are no acknowledgements.

Disclosure statement

No potential conflict of interest was reported by the author(s).

ORCID

N. W. Barasa http://orcid.org/0000-0003-4106-8629

Data availability statement

The data that support the findings of this study are openly available in Mendeley Data.(https://data.mendeley.com/drafts/dm94r5sx9c). DOI:10.17632/dm94r5sx9c.2

References

Ahmad, T., H. S. Mahmood, Z. Ali, M. A. Khan, and S. Zia. 2017. Design and development of a portable sisal decorticator. *Pakistan Journal of Agricultural Research* 30 (3):209–17. doi:10.17582/journal.pjar/2017.30.3.209.217.

Barasa, N., K. Njoroge, and T. Mbuya. 2021. An investigation of the effects of extraction and brushing variables on the properties of hedge sisal fibers using a raspador. *Journal of Natural Fibers* 1–20. doi:10.1080/15440478.2020.1870641.

Brenters, J. 2000. Design and financial assessment of small-scale sisal decortication technology in Tanzania. MSc, Eindhoven University of Technology.

Cantalino, A., E. Torres, and M. Silva. 2015. "Sustainability of sisal cultivation in Brazil using co-products and wastes." *Journal of Agriculture Science* 7 (7):64–74. doi:10.5539/jas.v7n7p64.

EPZ. 2005. *Kenya's Sisal Industry 2005 report*. Nairobi: Export Processing Zones Authority.

FAO. 2013. *Jute, kenaf, sisal, abaca, coir and allied fibres statistics*. Rome, Italy: FAO Corporate Document Repository.

Kanogu, H. M., A. V. Osore, and J. K. Kiguru. 2011. *Development of a sisal decortication for small holder farmers/traders: Redesign, fabrication and field testing*. Nairobi: University of Nairobi.

Kawongolo, J. B., J. Sentong-Kibalama, and L. Brown. 2002. Design of a decorticator for small scale sisal processing in Uganda. Presented at the ASAE Annual International Meeting/CIGR XVth World, Chicago,USA.

Kayumba, V. A., M. Bratveit, Y. Mashalla, and B. E. Moen. 2007. Acute respiratory symptoms among sisal workers in Tanzania. *Occupational Medicine* 57 (4):290–93. doi:10.1093/occmed/kqm004.

Kithiia, M. W., M. D. Munyasi, and M. S. Mutuli. 2020. Strength Properties of surface modified Kenyan sisal fibres. *Journal of Natural Fibers* 1–11. doi:10.1080/15440478.2020.1807446.

LSA (London Sisal Association). 2016. East African sisal fiber definitions. Accessed January 3, 2019. https://www.londonsisalassociation.org/kenya.php#

Majesh, M., and J. Pitchaimani. 2016. "Dynamic mechanical analysis and free vibration behavior of intra-ply woven natural fiber hybrid polymer composite." *Journal of Reinforced Plastics and Composites* 35 (2):28–42. doi:10.1177/0731684415611973.

Naik, K., R. P. Swamy, and P. Naik. 2014. Design and fabrication of areca fiber extraction machine. *International Journal of Emerging Technology and Advanced Engineering* 4:7.

Oduori, M. F. 2002. *Development and laboratory testing of a full-scale raspador decorticator*. Nairobi, Kenya: University of Nairobi.

Oduori, M. F. 2016. Design and experimental data on sisal decorticator laboratory model machine. University of Nairobi.

Oreko, B. U., S. Okiy, E. Emagbetere, and M. Okwu. 2018. Design and development of plantain fibre extraction machine. *Nigerian Journal of Technology (NIJOTECH)* 37 (2):397–406. doi:10.4314/njt.v37i2.14.

Petroudy, D. S. R. 2017. Physical and mechanical properties of natural fibers. In *Advanced high strength natural fibre composites in construction*, edited by M. Fan and F. Fu, 59–83. Iran: Elsevier. doi:10.1016/B978-0-08-100411-1.00003-0.

Phologolo, T., C. Yu, J. I. Mwasiagi, N. Muya, and Z. F. Li. 2012. Production and characterization of Kenyan sisal. *Asian Journal of Textile* 2 (2):17–25. doi:10.3923/ajtl.2012.17.25.

Roulunds, F. 2004. Design manual; the quality choice for any transmission. Denmark.

Shigley, J., C. Mischke, and T. Brown. 2004. *Standard handbook of machine design*. 3rd ed. Pennsylavania: McGraw Hill Professional.

Snyder, B. J., J. Bussard, J. Dolak, and T. Weister. 2006. A portable sisal decorticator for Kenyan farmers. *International Journal for Science Learning in Engineering* 2 (1):92–116.

Srinivasakumar, P. 2013. Sisal and its potential for creating innovative employment opportunities and economic prospects. *Journal of Mechanical and Civil Engineering (IOSR-JMCE)* 8 (6):1–8. doi:10.9790/1684-0860108.

UNIDO. 2001. *Past research results and present production practices in East Africa*. Viena: UNIDO. www.common-fund.org .

Van, G. J., and H. Toussaint. 1994. *Biomechanics: classical mechanics applied to human movement*. Armsterdam: Vrije University.

Zhu, Z., M. Hao, and N. Zhang. 2018. Influence of contents of chemical compositions on the mechanical property of sisal fibers and sisal fibers reinforced PLA composites. *Journal of Natural Fibers* 17 (1):101–12. doi:10.1080/15440478.2018.1469452.

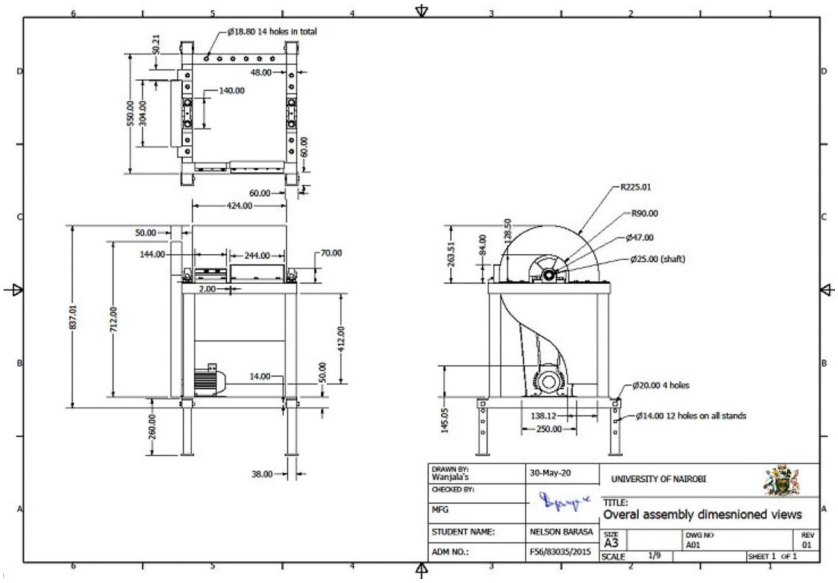

Figure A1. Views of the designed raspador.

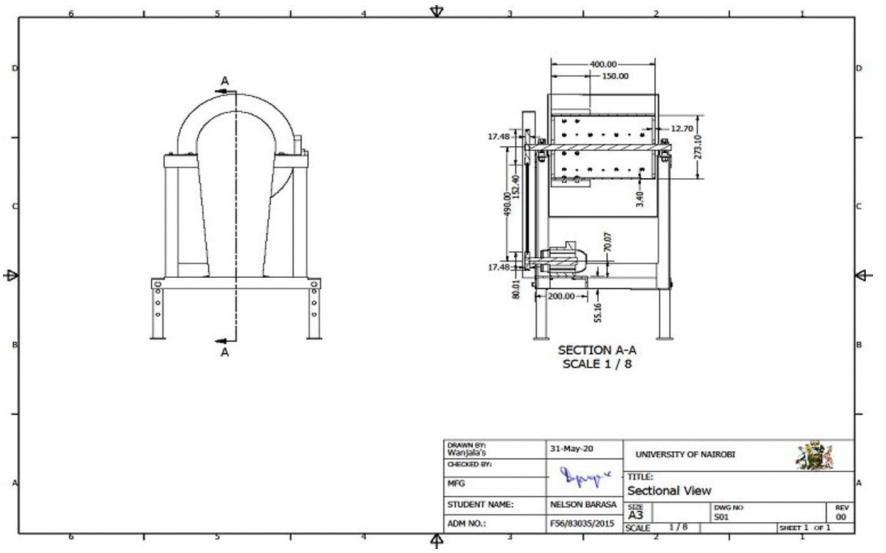

Figure A2. Sectional view.

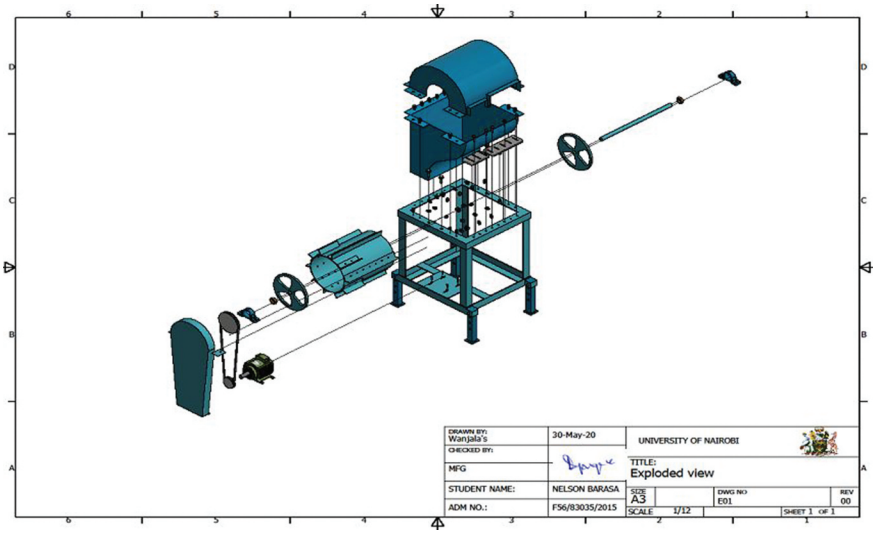

Figure A3. Exploded view.

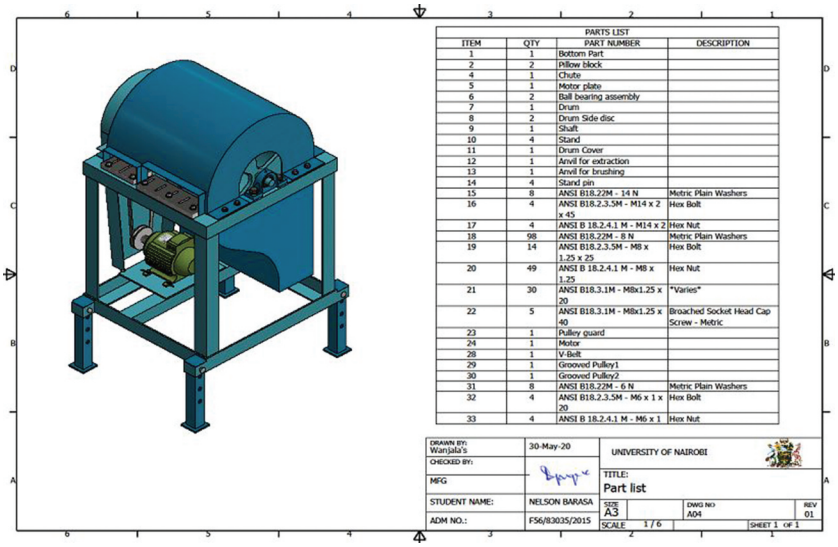

PARTS LIST			
ITEM	QTY	PART NUMBER	DESCRIPTION
1	1	Bottom Part	
2	2	Pillow block	
4	1	Chute	
5	1	Motor plate	
6	2	Ball bearing assembly	
7	1	Drum	
8	2	Drum Side disc	
9	1	Shaft	
10	4	Stand	
11	1	Drum Cover	
12	1	Anvil for extraction	
13	1	Anvil for brushing	
14	4	Stand pin	
15	8	ANSI B18.22M - 14 N	Metric Plain Washers
16	4	ANSI B18.2.3.5M - M14 x 2 x 45	Hex Bolt
17	4	ANSI B 18.2.4.1 M - M14 x 2	Hex Nut
18	98	ANSI B18.22M - 8 N	Metric Plain Washers
19	14	ANSI B18.2.3.5M - M8 x 1.25 x 25	Hex Bolt
20	49	ANSI B 18.2.4.1 M - M8 x 1.25	Hex Nut
21	30	ANSI B18.3.1M - M8x1.25 x 20	"Varies"
22	5	ANSI B18.3.1M - M8x1.25 x 40	Broached Socket Head Cap Screw - Metric
23	1	Pulley guard	
24	1	Motor	
28	1	V-Belt	
29	1	Grooved Pulley1	
30	1	Grooved Pulley2	
31	8	ANSI B18.22M - 6 N	Metric Plain Washers
32	4	ANSI B18.2.3.5M - M6 x 1 x 20	Hex Bolt
33	4	ANSI B 18.2.4.1 M - M6 x 1	Hex Nut

Figure A4. Part list.

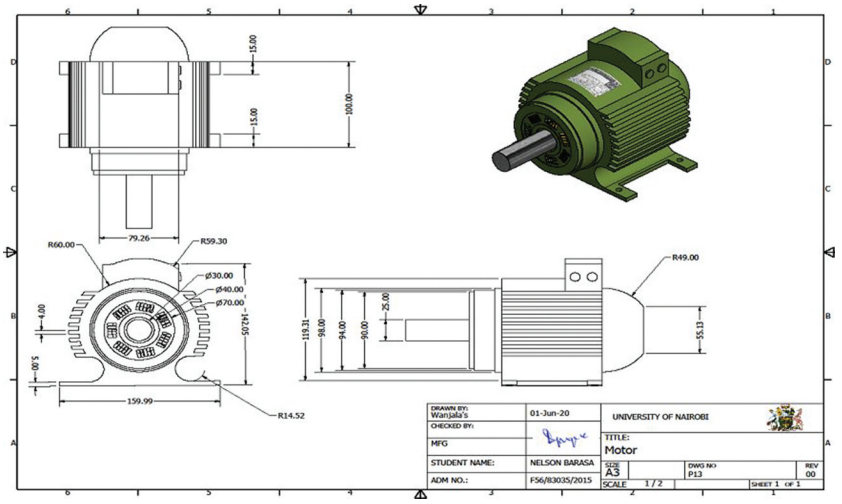

Figure A5. Motor.

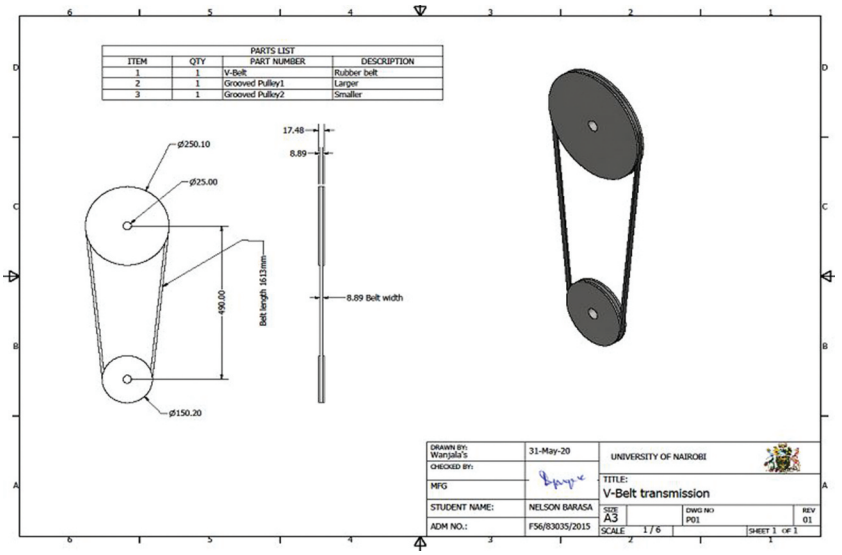

Figure A6. Belt drive.

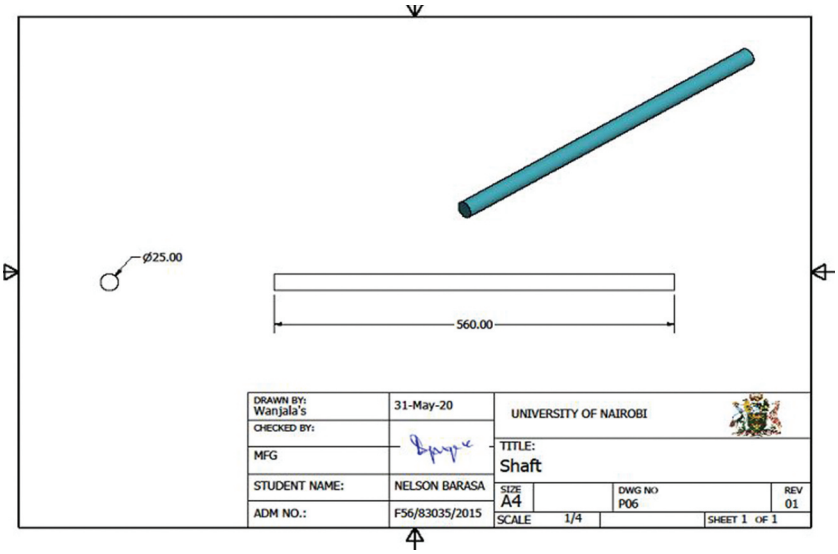

Figure A7. Shaft.